Supporting Information for "Highly Sensitive Mid-Infrared Photodetector Enabled by Plasmonic Hot Carriers in the First Atmospheric Window"

Yuan-Fang Yu(于远方)[1], Ye Zhang(张也)[2], Fan Zhong(仲帆)[2], Lin Bai(白琳)[1], Hui Liu(刘辉)[2], Jun-Peng Lu(吕俊鹏)[1]* and Zhen-Hua Ni(倪振华)[1]*

[1]School of Physics, Southeast University, Nanjing 211189, China
[2]National Laboratory of Solid State Microstructures & School of Physics, Collaborative Innovation Center of Advanced Microstructures, Nanjing University, Nanjing 210093, China

1. Morphology of the fabricated AZO disc arrays

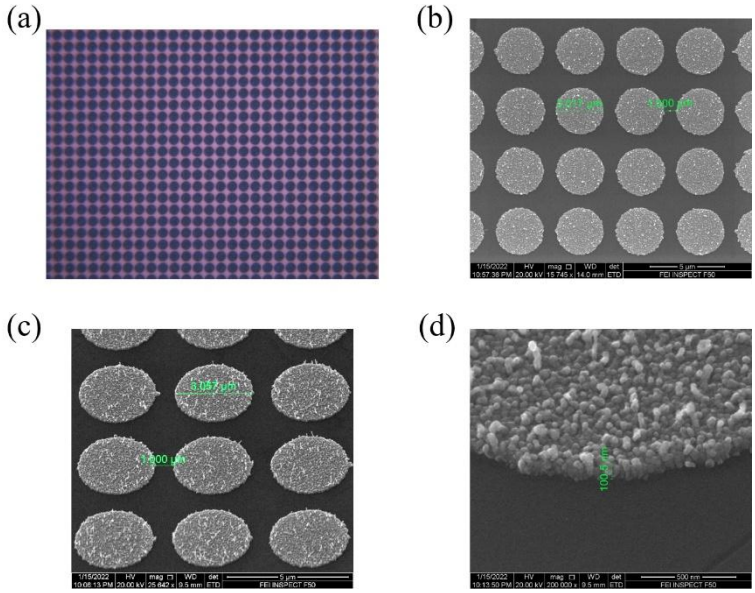

Fig. S1. (a) Optical image of AZO disc arrays on SiO_2/Si substrate. The diameter of AZO disc is 3μm. (b) SEM images AZO disc arrays on SiO_2/Si substrate with size measured. (c) SEM images AZO disc arrays observed along a certain tilt angle. (d) Thickness measurements of AZO disc.

2. The generation rate of hot electrons

The generation rate of hot electron is mainly relative to the energy of incident photons, electric field in nanostructures, and Fermi level. The generation rate of hot electrons can be calculated according to the equation below[1],

$$Rate_{HE} = \frac{2}{\pi^2} \times \frac{e^2 {E_F}^2}{\hbar} \frac{1}{(\hbar\omega)^3} \int_{S_{NC}} \left| E_{normal}(\theta, \varphi) \right|^2 ds \qquad \text{(S1)}$$

Where $E_{normal}(\theta, \varphi)$ is the component of electric field normal to the nanostructures' surface, inside the materials, and the integral is taken over the whole surface. E_F is the Fermi energy of AZO. $\hbar\omega$ is the photon energy.

3. Raman spectra of G band and 2D band

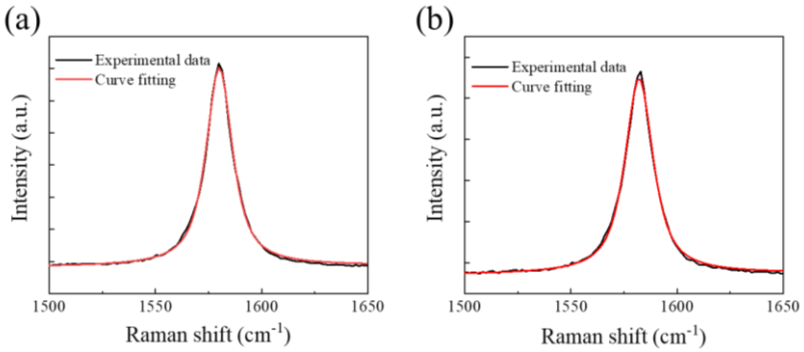

Fig. S2 (a) Raman G band of pristine bi-layer graphene, red line is the fitting curve of experimental data. (b) Raman G band of AZO/bi-layer graphene heterostructure, red line is the fitting curve of experimental data.

Table S1. Detail fitting results of the Raman G band for the bi-layer graphene and AZO/bi-layer graphene heterostructure

	Center (cm^{-1})	Width	Height
Bi-layer Graphene	1580	15	12367
AZO/bi-layer Graphene	1582	16	9514

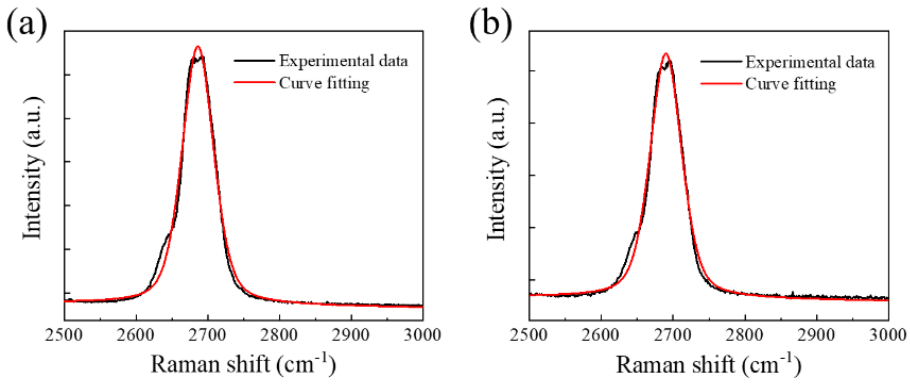

Fig. S3. (a) 2D band of pristine bi-layer graphene, red line is the fitting curve of experimental data. (b) 2D band of AZO/bi-layer graphene heterostructure, red line is the fitting curve of experimental data.

Table S2. Detail fitting results of the Raman 2D band for the bi-layer graphene and AZO/bi-layer graphene heterostructure

	Center (cm^{-1})	Width	Height
Bi-layer Graphene	2686	52	11845
AZO/bi-layer Graphene	2690	52	9372

4. Performance of AZO/bi-layer graphene photodetector at 3.5 μm and 4 μm, operated at room temperature

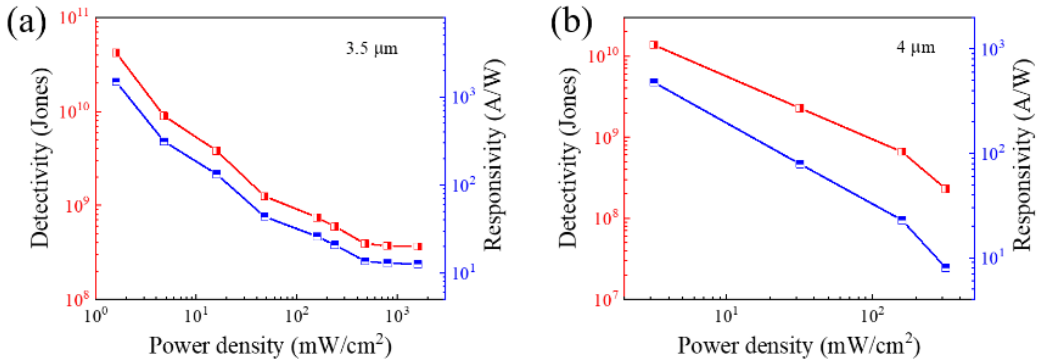

Fig. S4. (a) Detectivity and responsivity of AZO/bi-layer graphene photodetector as a function of power density at 3.5 μm. V_{ds} = 0.5 V, V_g = 0V. (b) Detectivity and responsivity of AZO/bi-layer graphene photodetector as a function of power density at 4 μm. V_{ds} = 0.5 V, V_g = 0V.

5. EQE of AZO/bi-layer graphene photodetector at room temperature

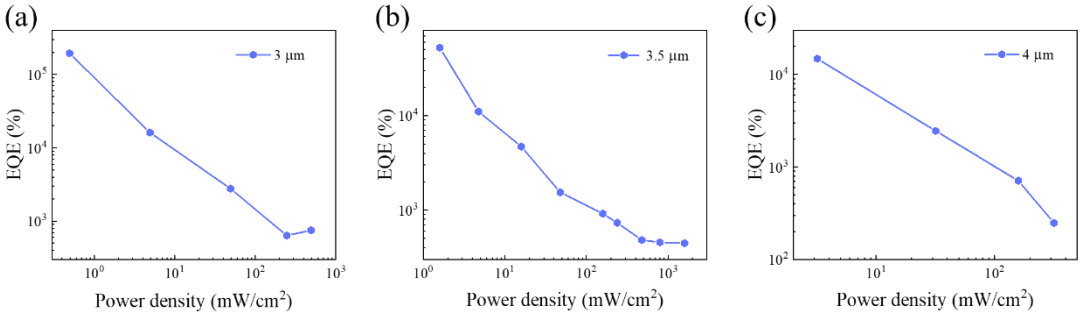

Fig. S5. EQE of AZO/bi-layer graphene photodetector as a function of power density at the wavelengths of 3 μm (a), 3.5 μm (b) and 4 μm (c). V_{ds} = 0.5 V, V_g = 0V.

Reference

[1] Liu T J, Besteiro L V, Wang Z M and Govorov A O 2019 *Faraday Discuss.* **214** 199